Wang, P, Hawkins, T, Richardson, C, Cummins, I, Deeks, M, Sparkes, I, Hawes, C and Hussey, P (2014)

The plant cytoskeleton, NET3C and VAP27 mediates the link between the plasma membrane and endoplasmic reticulum

Current Biology, 24 (12). pp. 1397-1405.
10.1016/j.cub.2014.05.003

The plant cytoskeleton, NET3C and VAP27 mediates the link between the plasma membrane and endoplasmic reticulum

Pengwei Wang[1], Timothy J. Hawkins[1], Christine Richardson[1], Ian Cummins[1], Michael J. Deeks[1#], Imogen Sparkes[2#], Chris Hawes[2] and Patrick J. Hussey[1*]

[1] School of Biological and Biomedical Sciences, University of Durham, South Road, Durham, DH1 3LE, UK

[2] Department of Biological and Medical Sciences, Oxford Brookes University, Gipsy Lane, Headington, Oxford, OX3 0BP, UK

[#] Current address: Biosciences, College of Life and Environmental Sciences, University of Exeter, Stocker Road, Exeter, EX4 4QD, UK

*Corresponding author: p.j.hussey@durham.ac.uk

Summary

The cortical endoplasmic reticulum (ER) network in plants is a highly dynamic structure and it contacts the plasma membrane (PM) at ER/PM anchor/contact sites. These sites are known to be essential for communication between the ER and PM for lipid transport, calcium influx and ER morphology in mammalian and fungal cells. The nature of these contact sites is unknown in plants [1, 2] and here we have identified a complex that forms this bridge. This complex includes (i) NET3C which belongs to a plant specific super-family (NET) of actin-binding proteins [3]. (ii) VAP27, a plant homologue of the yeast Scs2 ER/PM contact site protein [4, 5] and (iii) the actin and microtubule networks. We demonstrate that NET3C and VAP27 localise to punctae at the PM, that NET3C and VAP27 form homodimers/oligomers and together form complexes with actin and microtubules. We show that F-actin modulates the turnover of NET3C at these punctae and microtubules regulate the exchange of VAP27 at the same sites. Based on these data, we propose a model for the structure of the plant ER/PM contact sites.

Highlights

1. NET3C belongs to a plant specific NET super-family.
2. NET3C links the actin cytoskeleton to ER/PM contact/anchor sites.
3. VAP27 is phylogenetically conserved and interacts with NET3C.
4. A novel complex for plant ER/PM contact site is identified from our study.

Results and Discussion

NET3C localises to ER/PM-associated punctae.

The actin cytoskeleton is a dynamic filament network that is involved in many cellular processes [6, 7]. In plants, it plays a unique role in organelle movement and endomembrane trafficking [8, 9], a role normally played by microtubules in animals [10, 11]. However, we know little about the proteins that are involved in linking the actin cytoskeleton to the plant endomembrane system. For example, it is known that the actin cytoskeleton is involved in ER movement but how they are linked is still an enigma. [12]. Substances made in the ER are transported to various destinations through vesicular trafficking pathways [13]. Although, direct association between ER and other membrane compartments also exists, which may provide alternative routes for material transport [14, 15]. In this context, the ER and PM are connected via ER/PM anchor/contact sites/junctions [16-19] but the nature of these sites in plants is unknown.

NET3C belongs to a plant specific NET super-family, which is a group of proteins that link the actin cytoskeleton to specific endomembrane compartments [3].The protein contains two functional domains (Figure 1A); a NAB (NET-Actin-Binding, a.a.1-94) domain and a coiled-coil domain (a.a.139-194). Here we show that NET3C binds F-actin. An actin co-sedimentation assay was performed using leaf extracts from *N. benthamiana* expressing GFP-NET3C. NET3C was found in the pellet fraction (lane4) in the presence of F-actin (Figure 1F). When expressed in *N. benthamiana* leaves, GFP-NET3C gave a 'beads on a string' localisation, which is a characteristic of members of the NET superfamily [3] (Figure 1B-D). The beads represent numerous immobile punctae (0.25-1.0μm) that appear to

associate with the ER (Figure 1B; Movie S1). These NET3C punctae resemble the ER punctae that were previously suggested to be putative ER/PM contact sites [1, 2, 20]

The association of NET3C punctae with the ER membrane was found to be independent of the actin cytoskeleton; 87.9±10.1% of NET3C punctae associated with the ER (Figure 1B) and when the cells were treated with the actin depolymerizing drug latrunculin B (Figure 1C), this association did not change significantly (87.4±8.3%; p=0.47). NET3C punctae are F-actin associated with 92.0±3.1% contacting the actin network (RFP-Lifact; Figure 1D). The NET3C punctae that are associated with the ER or F-actin compared to non-associated is significantly different (chi-square tests, $p<0.01$; Figure S1 A-C).

This association is further emphasized by showing that the turnover of NET3C punctae as assessed by FRAP, is influenced by F-actin but not by microtubules. The recovery of GFP-NET3C in the photo-beached region was enhanced significantly from 44.6±12.1% to 77.6±18.5% (max recovery, $p=1.03x10^{-7}$) when treated with latrunculin B (Figure 1E). In contrast, treatment of the cells with the microtubule depolymerizing drug, oryzalin, had little effect on NET3C turnover. These data indicate that NET3C localization is independent of F-actin but that once the punctae are attached to the F-actin, the exchange of NET3C is restrained.

As the ER association of NET3C is independent of actin and the interaction with actin is at the N-terminus of NET3C, we assessed whether the C-terminus is responsible for membrane localization. A NAB domain deleted NET3C was generated (NET3CΔNAB) and this is shown to localize to the ER and PM (Figure S1D-F), confirming that the C-terminus is essential for membrane localization. In addition, NET3C lacking the C-terminal sequence (NET3CΔC-term) did not associate with either F-actin or membrane compartments (Figure S1G).

In order to confirm that the localization of the GFP-NET3C in transiently expressing *N. benthamiana* cells is similar to the intracellular localization of native NET3C in Arabidopsis, immunofluorescence studies were performed

using anti-NET3C. Western-blotting using anti-NET3C identified a single band of the appropriate molecular weight in Arabidopsis cell extracts (Figure S1I).

Immunofluorescence was performed on Arabidopsis root tips expressing either GFP-HDEL(ER) or GFP-FABD2 (F-actin). Anti-NET3C labeled punctate structures that closely associate with the ER (96.4±5.6%, Figure 1H) and F-actin (96.2±7.3%, Figure S1H) at the cell cortex. Furthermore, immuno-gold labeling of Arabidopsis root tips showed gold particles at the PM in close proximity with the ER (Figure S1K) as well as at putative ER/PM contact sites (Figure 1G). The enrichment of anti-NET3C gold beads at the PM was confirmed statistically using chi-square tests (Figure S1L). These results on endogenous NET3C are consistent with the tobacco transient expression (Figure 1B), and confirm that NET3C is specifically found at punctae at the PM and putative ER/PM contact sites. Furthermore a double mutant, *NET3C RNAi/net3b* is shown to be gamete lethal indicating that NET3B/C are essential genes. (Figure S2C-F)

Studies in yeast have suggested that C-terminal basic motifs (lysine/arginine residues) in many proteins are required for phospholipid binding [21]. The sequence of the NET3C C-terminus encodes several lysine residues, including a lysine at position 211 (Figure 2A). A mutant where the lysine is substituted for alanine (GFP-NET3C K211A) was generated. This mutant is still able to form punctae that associate with F-actin and the ER (Figure 2B & F). However, most are mobile, which indicates that PM association is reduced (Movie S2). The ratio of fluorescence intensity at the cell cortex to the nucleoplasm was determined to be 10.9±4.1 (arbitrary units) for NET3C and 0.88±0.86 for NET3C-K211A (Figure 2E), indicating that the fluorescent signal for NET3C K211A accumulated in the nucleus, a feature of many cytoplasmic protein/FP constructs. [22, 23](Figure 2C-D).

When the GFP-NET3CΔNAB mutant, which on its own is evenly distributed on the ER and PM (Figure S1D), was expressed with full length RFP-NET3C, the deletion mutant was recruited to the punctae identified by the RFP-NET3C (Figure 2G). This indicates that native NET3C may exist as a dimer/oligomer through an interaction between the C-terminal sequences. This interaction was

confirmed by immunoprecipitation (Figure 2H) and FRET-FLIM experiments. In the FRET-FLIM, the lifetime of GFP-NET3C was found to be 2.21±0.03ns in the presence of RFP-NET3C, which is significantly reduced (by 0.24ns) when compared to GFP-NET3C on its own (2.45±0.03ns, $p=9.07x10^{-7}$), indicating a physical interaction [24, 25]. In comparison, the lifetime of the GFP-RFP fusion positive control was found to be 2.14±0.06ns (Figure 2I).

These data suggest a model where the NET3C dimerises/oligomerises at the C-terminal ends, the C-terminus binds the puncta to the membrane and the N-terminus binds F –actin. The association between NET3C and the PM is likely to be through direct lipid binding via the C-terminal basic motif or alternatively, through the interaction with other membrane localised proteins. NET3C is also likely to form anti-parallel dimers/oligomers that link the ER and PM as GFP-NET3CΔNAB localizes to the ER and PM. F-actin appears to stabilize the association of NET3C.(Figure 2J).

VAP27 localises to ER/PM contact sites

VAPs are phylogenetically conserved proteins [26-29]. They comprise a C-terminal transmembrane domain (a.a.234-253), an N-terminal major sperm domain (a.a.1-129) and a coiled-coil domain (a.a.178-234; Figure 3A). VAP27-YFP expressed in *N. benthamiana* leaves localises to the ER network as well as immobile punctate structures (0.25-1.2μm; Figure 3B), reminiscent of the putative ER/PM anchor sites observed in previous studies [1, 2] and in other organisms [17, 19]. These punctae are stationary while the majority of the ER network remodels (Figure S3A; Movie S3A). The VAP27-YFP punctae are located along ER tubules but not generally associated with three way junctions (Figure 3B). Stable Arabidopsis lines expressing VAP27-GFP under its endogenous promoter were generated, and the same ER associated punctae were identified (Figure S3B, Movie S3B). At the ultrastructural level, in Arabidopsis expressing VAP-27-YFP, attachment sites of the ER to PM were found. The sites are 0.5-1.0 μm, consistent with the size of VAP27 punctae observed using light microscopy (Figure S3C).

Yeast Scs2p is a known ER/PM contact site protein [4, 5, 16] and has 54% similarity to full length VAP27 (Figure S3E). When expressed in plants, Scs2p-GFP co-localized with VAP27-YFP at the ER and the putative ER/PM contact sites (Figure S3D). However, the Scs2p labeled ER/PM contact sites were less distinct, presumably because the two proteins compete at the same site. This result suggests that Scs2p co-localizes with VAP27 at equivalent ER/PM contact sites in plants.

Statistical analysis shows that 81.2±9.4% of VAP27-YFP labeled ER/PM contact sites associated with F-actin (GFP-Lifeact), whereas 59.5±4.3% were found to associate with KMD-RFP labeled microtubules[30] (Figure 3C-D). FRAP was used to study the dynamics of VAP27 turnover. ER membrane proteins (calnexin-GFP) exhibit a fast recovery at the ER cisternae ($T_{1/2}$=1.8-2.2 seconds) and has a large mobile fraction (Rmax=86-89%; Figure S3F). However, the recovery of VAP27-YFP at the ER/PM contact site was slow in comparison, with the maximum recovery reduced to 54.1±12.6% and a half-time of recovery of 15.0±7.6 seconds. The slow recovery suggests that VAP27 is part of a protein complex that affects its mobility. In addition, the turnover of VAP27-YFP dramatically increased when microtubules were depolymerized (Rmax=70.3±12.6%, p=0.006), indicating that VAP27 has some functional association with microtubules. On the other hand, recovery was unaffected when F-actin was removed (Rmax=49.9±10.4%; Figure 3E). These data indicate that the microtubule network has an impact on the dynamics of VAP27 at the ER/PM contact sites.

To further confirm an interaction between VAP27 and microtubules, total protein extracts from *N. benthamiana* leaves expressing VAP27-mRFP were co-incubated with microtubules and the mixture subjected to centrifugation. VAP27-mRFP was only detected in the pellet in the presence of microtubules (Figure 3F), confirming an interaction *in vitro*. This finding is consistent with the FRAP data described above. In conclusion, VAP27 is part of the ER/PM contact sites in plants and it associates with microtubules that constrain its mobility.

In addition, VAP27 is able to form dimers/oligomers *in vivo* like its mammalian equivalent[27], which was confirmed by immunoprecipitation (Figure S3G) and FRET-FLIM (Figure 3G). The lifetime of VAP27-GFP was reduced by 0.42ns to 2.06±0.1ns when co-expressed with VAP27-RFP which is significantly different from the VAP27-GFP control (2.48±0.04ns), indicating a physical interaction.

NET3C interacts with VAP27 at the ER/PM contact sites

The localisations of NET3C and VAP27 appear similar so we performed colocalisation studies. VAP27-YFP was co-expressed with CFP-HDEL (ER) and RFP-NET3C in *N. benthamiana* leaves and the results show that they co-localise at the ER/PM contact sites (Figure 4A). Interestingly, yeast Scs2-YFP also co-localised with NET3C at these contact sites, which further indicates that the localization of Scs2 in plant cells is the same as VAP27 (Figure S4A).

To investigate whether VAP27 and NET3C interact we used co-immunoprecipitation and FRET-FLIM. RFP-NET3C was found in the pellet fraction only when co-expressed with VAP27-YFP (Figure S4B) and the fluorescence lifetime of GFP-VAP27 was reduced by 0.29ns to 2.13±0.06 in the presence of RFP-NET3C compared to control (2.42ns±0.02). These data indicate a close association of NET3C/VAP27 *in vivo* (Figure 4B). Furthermore, immunostaining an Arabidopsis line stably transformed with 35S:VAP27-YFP using anti-NET3C and anti-GFP, showed that VAP27 punctae were also labeled with the NET3C antibody (Figure S4C).

The major sperm domain of VAP27 is conserved (Figure S3E) and previous studies suggest that a lysine residue at position 58 and two tyrosine residues at position 59/60 are necessary for VAP to interact with other proteins [29]. We mutated the lysine 58 and tyrosine 59/60 to asparagine and alanine respectively. The resulting mutants were still ER localised but failed to label any ER/PM contact sites (Figure 4C & S4D). Moreover, the mutants did not appear to co-localise with NET3C. This suggests that the mutation of these residues in the major sperm domain prevents the NET3C/VAP27 interaction and ER/PM association (Figure 4D).

Further mutagenesis was performed at the NET3C C-terminus (Figure 2A). Substitution of phenylalanine residues at positions 209 and 210 with alanine did not affect its interaction with VAP27 (Figure S4G). However, the association of NET3C F209/210A labelled punctae with F-actin was enhanced (Figure S4E-F), and the ER network was distorted (Figure S4H). In addition, the structure of VAP27 labelled ER/PM contact sites was also affected, as they became more mobile in the presence of NET3C F209/210A (Movie S5). These results suggest that specific residues at the C-terminus are essential for the association of NET3C with F-actin and membrane and they also appear to be important for maintaining ER structure.

NET3C-VAP27, Microtubule and Actin Model

Here we demonstrate that NET3C, VAP27 and the cytoskeleton are involved in organizing ER/PM contact/anchor sites (Figure 4E). We suggest two possible structural models explaining this association: (i) VAP27 may directly link the ER and PM and interact with PM/ER associated NET3C and as yet unknown PM proteins (Figure 4F). The actin and microtubule networks fix NET3C and VAP27 respectively at the contact sites; (ii) NET3C forms a pre-existing platform with other unknown proteins at the ER/PM and VAP27 is recruited to these sites upon certain signal stimuli or protein modification (Figure 4G). In both cases the cytoskeleton is responsible for stabilizing NET3C and VAP27 at the contact sites.

Figure legends

Figure 1. NET3C localises to PM/ER contact sites and F-actin.

(a) Diagrammatic illustration of the GFP-NET3C fusion; NET actin binding domain (a.a.1-a.a.94) and coiled-coil domain (a.a.139-a.a.194). **(B)** GFP-NET3C labelled immobile punctae co-locate along the ER (red) in leaf epidermal cells. NET3C punctae were associated (87.8 ± 10.1% of association) with the persistent ER nodules that are known as ER/PM contact sites (high magnification inset). **(C)** NET3C associates with the PM/ER contact sites independent of F-actin. When cells were treated with latrunculin (Lat B), NET3C punctae were associated with the ER network (87.4% ± 8.3 association). **(D)** NET3C punctae associate with F-actin (RFP-Lifact) producing a typical beads-on-string pattern (high magnification inset). Statistical analysis of NET3C punctae and F-actin association indicates a strong correlation (92.8 ± 3.1%). **(E)** Fluorescence-recovery after photobleaching (FRAP) of GFP-NET3C with different drug treatments. The mobility of GFP-NET3C was enhanced (reflected by an increase of max recovery) when actin filaments were removed with Lat B ($p=1.03x10^{-7}$). Little difference was found between oryzalin treatment (to remove microtubules) and the control (p=0.791). **(F)** Western blot probed with GFP-antibody showing co-sedimentation of GFP-NET3C with actin-filaments. After ultra-centrifugation, the supernatant (S) and pellet (P) fractions of GFP-NET3C with and without F-actin were fractionated on a gel. GFP-NET3C was found in the pellet fraction in the presence of F-actin. Lane 1, GFP-NET3C alone (S); Lane 2, GFP-NET3C alone (P); Lane 3, GFP-NET3C + F-actin (S); Lane 4, GFP-NET3C + F-actin (P). **(G)** Immuno-gold labeling of sections taken through Arabidopsis root tips using anti-NET3C showing NET3C associates with the PM as well as the ER/PM junctions. Gold particles were enhanced (larger dots overlaid on the original gold particles) using Photoshop for better visualisation. **(H)** Immuno-fluorescence of GFP-HDEL (ER marker) expressing Arabidopsis root tips with NET3C and GFP antibodies. Endogenous NET3C labels punctae and associates with the ER (96.4±5.6% association; scale bar = 10 μm for confocal; scale bar = 100 nm for TEM).

Figure 2. NET3C is able to self-interact and is recruited to the plasma membrane via the C-terminus.

(A) Diagrammatic illustration of NET3C showing the last ten amino, two phenoanalines (FF) are found at position 209/210 and a lysine (K) at 211. **(B**) Site-direct mutation of the C-terminal putative lipid binding motif on NET3C. GFP-NET3C K211A, which became

more cytoplasmically localised, labeled F-actin and mobile punctae. **(C) & (D)** Nuclear accumulation of GFP-NET3C K211A was found compared to control, indicating an enhanced cytoplasmic pool. The fluorescence intensity at the cell cortex and nuclear region are shown on the image. **(E)** Fluorescence ratio of cell cortex to nucleus . A high ratio (10.9±4.1) was found for GFP-NET3C, whereas a low ratio (0.88±0.86) was found with GFP-NET3C K211A. **(F)** Punctae labeled with GFP-NET3C K211A were still F-actin and ER associated. **(G)** GFP-NET3CΔNAB was recruited to the punctae when co-expressed with RFP-NET3C, suggesting that NET3C may self-interact through its C-terminal sequence. **(H)** Immuno-precipitation of RFP-NET3C and GFP-NET3C using a RFP antibody. GFP-NET3C was only found in the pellet fraction in the presence of RFP-NET3C (lane 1 and 2) indicating that the protein is able to self-interact. **(I)** FRET-FLIM analysis of NET3C interactions. Images were pseudo-coloured according to the GFP lifetime. The lifetime of GFP-NET3C (donor alone) was measured at 2.45±0.03 ns, whereas the lifetime of GFP was significantly reduced to 2.21±0.09 ns ($p=9.07x10^{-7}$) in the presence of RFP-NET3C (acceptor), suggesting NET3C is able to self-interact. In contrast, the positive control (GFP linked directly to RFP) had an average lifetime of 2.14±0.04 ns, indicating that a ca. 0.3ns reduction is found in a close association. The value of x^2 is close to 1 (indicative of good curve fitting) for all measurements. Please note that the peak of the lifetime frequency shifted to the left when the average fluorescence lifetime was reduced. **(J)** Diagram of possible plasma membrane recruitment of NET3C. NET3C dimer/oligomer binds to the PM or ER membrane via its C-terminus and binds to F-actin through the N-terminal NAB domain (I). NET3C could possibly form antiparallel dimers/oligomers that bridge between ER/PM (III). The K211A mutation prevents the membrane association of NET3C (II)&(IV) (scale bar = 10 μm).

Figure 3. VAP27 is an ER membrane protein and also localises to PM/ER contact sites

(A) Diagrammatic illustration of the VAP27-YFP fusion; major sperm domain (a.a.1-a.a.129), coiled-coil domain (a.a.178-a.a.234) and transmembrane domain (a.a.234-a.a.253). **(B)** VAP27-YFP localizes to the ER as well as PM/ER contact sites, Calnexin-GFP is a marker for the ER membrane (high magnification inset). **(C)** VAP27-YFP punctae at the ER/PM contact sites associate with F-actin (GFP-Lifact; 81.2±9.4% co-alignment; high magnification inset). **(D)** VAP27-YFP punctae associate with microtubules (KMD-RFP is the marker). Statistical analysis indicates a moderate ratio of co-alignment

(59.5±4.3%; high magnification inset). **(E)** Fluorescence-recovery after photobleaching (FRAP) of VAP27-YFP at the PM/ER contact sites following different drug treatments. The mobility of VAP27-YFP did not chang when actin filaments were removed with LAT B (p=0.465). A significant increase (reflected BY an increase in max recovery) was found with oryzalin treatment (p=0.006). **(F)** Western blot probed with RFP-antibody showing co-sedimentation of VAP27-mRFP with microtubules. After ultra-centrifugation, the supernatant (S) and pellet (P) fractions in the presence or absence of microtubules were run on the gel. VAP27 was found in the pellet fraction in the presence of microtubules. Lane 1, VAP27-RFP + MT (S); Lane 2, VAP27-RFP + MT (P); Lane 3, VAP27-RFP alone (S); Lane 4, VAP27-RFP alone (P). **(G)** FRET-FLIM analysis of VAP27 interaction. The lifetime of VAP27-GFP (donor alone) was measured at 2.48±0.04ns, whereas the lifetime of GFP was significantly reduced to 2.06±0.01ns ($p=3.49 \times 10^{-9}$) in the presence of VAP27-RFP (scale bar = 10 μm).

Figure 4. VAP27 interacts with NET3C.

(A)The ER network was labeled by CFP-HDEL and RFP-NET3C co-localised with VAP27-YFP at the ER/PM contact sites. **(B)** FRET-FLIM analysis of the NET3C/VAP27 interaction. GFP-VAP27 has a lifetime of 2.42±0.02ns on its own. The fluorescence lifetime of GFP-VAP27 was reduced to 2.13±0.06 ns ($p=1.23 \times 10^{-12}$) when co-expressed with RFP-NET3C, indicating an interaction between the two proteins. **(C)** Site-directed mutation in the major sperm domain. VAP27 T59/60A was still found at the ER network but failed to concentrate at the ER/PM contact site and to colocalise with RFP-NET3C. **(D)** Propose illustration of VAP27-PM association. Point mutations on the major sperm domain prevent VAP27 associating with PM/ER contact site. **(E)** Diagram showing VAP27 (at the ER) interacting with NET3C (at the PM), forming a stationary complex at the ER/PM contact site. The cytoskeleton was found associated with these complexes interacting with NET3C and VAP27. Two possible models are suggested: **(F)** VAP27 may directly link the ER/PM and interact with PM associated NET3C.;**(G)** Alternatively, NET3C may form a pre-existing platform with other proteins at the plasma membrane. In addition to NET3C and VAP27, other proteins may also be required for the function and structure of ER/PM contact sites (scale bar = 10 μm).

Accession number

The Arabidopsis genome accession number for NET3C is At2g47920 and for VAP27 it is At3g60600.

Acknowledgements

We thank Dr Andrei Smertenko for helping with the microtubule co-sedimentation assay. We also thank Patrick Duckney for providing the GFP-RFP construct. The work was supported by a BBSRC grant (BB/G006334/1) to P.J.H. and preliminary work on VAP27 was supported by a Leverhulme trust grant (F/00382/G) to C.H.

Author Contributions

P.W. performed the experiments.. T.J.H., I.C. , M.J.D, C.R., and IS contributed data and helped in the analysis. P.W., C.H. and P.J.H. wrote the manuscript.

References

1. Sparkes, I., Runions, J., Hawes, C., and Griffing, L. (2009). Movement and remodeling of the endoplasmic reticulum in nondividing cells of tobacco leaves. Plant Cell *21*, 3937-3949.
2. Sparkes, I., Hawes, C., and Frigerio, L. (2011). FrontiERs: movers and shapers of the higher plant cortical endoplasmic reticulum. Curr Opin Plant Biol *14*, 658-665.
3. Deeks, M.J., Calcutt, J.R., Ingle, E.K., Hawkins, T.J., Chapman, S., Richardson, A.C., Mentlak, D.A., Dixon, M.R., Cartwright, F., Smertenko, A.P., et al. (2012). A superfamily of actin-binding proteins at the actin-membrane nexus of higher plants. Curr Biol *22*, 1595-1600.
4. Stefan, C.J., Manford, A.G., Baird, D., Yamada-Hanff, J., Mao, Y., and Emr, S.D. (2011). Osh proteins regulate phosphoinositide metabolism at ER-plasma membrane contact sites. Cell *144*, 389-401.
5. Loewen, C.J., Young, B.P., Tavassoli, S., and Levine, T.P. (2007). Inheritance of cortical ER in yeast is required for normal septin organization. J Cell Biol *179*, 467-483.
6. Hussey, P.J., Ketelaar, T., and Deeks, M.J. (2006). Control of the actin cytoskeleton in plant cell growth. Annu Rev Plant Biol *57*, 109-125.
7. Smertenko, A.P., Deeks, M.J., and Hussey, P.J. (2010). Strategies of actin reorganisation in plant cells. J Cell Sci *123*, 3019-3028.
8. Boevink, P., Oparka, K., Santa Cruz, S., Martin, B., Betteridge, A., and Hawes, C. (1998). Stacks on tracks: the plant Golgi apparatus traffics on an actin/ER network. Plant J *15*, 441-447.
9. Ueda, H., Yokota, E., Kutsuna, N., Shimada, T., Tamura, K., Shimmen, T., Hasezawa, S., Dolja, V.V., and Hara-Nishimura, I. (2010). Myosin-dependent endoplasmic reticulum motility and F-actin organization in plant cells. Proc Natl Acad Sci U S A *107*, 6894-6899.
10. Klopfenstein, D.R., Kappeler, F., and Hauri, H.P. (1998). A novel direct interaction of endoplasmic reticulum with microtubules. The EMBO journal *17*, 6168-6177.
11. Watson, P., Forster, R., Palmer, K.J., Pepperkok, R., and Stephens, D.J. (2005). Coupling of ER exit to microtubules through direct interaction of COPII with dynactin. Nat Cell Biol *7*, 48-55.
12. Sparkes, I.A., Frigerio, L., Tolley, N., and Hawes, C. (2009). The plant endoplasmic reticulum: a cell-wide web. Biochem J *423*, 145-155.
13. Bonifacino, J.S., and Glick, B.S. (2004). The mechanisms of vesicle budding and fusion. Cell *116*, 153-166.
14. Schattat, M., Barton, K., Baudisch, B., Klosgen, R.B., and Mathur, J. (2011). Plastid stromule branching coincides with contiguous endoplasmic reticulum dynamics. Plant physiology *155*, 1667-1677.
15. de Brito, O.M., and Scorrano, L. (2008). Mitofusin 2 tethers endoplasmic reticulum to mitochondria. Nature *456*, 605-610.
16. Manford, A.G., Stefan, C.J., Yuan, H.L., Macgurn, J.A., and Emr, S.D. (2012). ER-to-plasma membrane tethering proteins regulate cell signaling and ER morphology. Dev Cell *23*, 1129-1140.
17. Varnai, P., Toth, B., Toth, D.J., Hunyady, L., and Balla, T. (2007). Visualization and manipulation of plasma membrane-endoplasmic reticulum contact sites indicates the presence of additional molecular components within the STIM1-Orai1 Complex. J Biol Chem *282*, 29678-29690.

18. Luik, R.M., Wang, B., Prakriya, M., Wu, M.M., and Lewis, R.S. (2008). Oligomerization of STIM1 couples ER calcium depletion to CRAC channel activation. Nature *454*, 538-542.
19. Giordano, F., Saheki, Y., Idevall-Hagren, O., Colombo, S.F., Pirruccello, M., Milosevic, I., Gracheva, E.O., Bagriantsev, S.N., Borgese, N., and De Camilli, P. (2013). PI(4,5)P(2)-dependent and Ca(2+)-regulated ER-PM interactions mediated by the extended synaptotagmins. Cell *153*, 1494-1509.
20. Sparkes, I.A., Ketelaar, T., de Ruijter, N.C., and Hawes, C. (2009). Grab a Golgi: laser trapping of Golgi bodies reveals in vivo interactions with the endoplasmic reticulum. Traffic *10*, 567-571.
21. Scheglmann, D., Werner, K., Eiselt, G., and Klinger, R. (2002). Role of paired basic residues of protein C-termini in phospholipid binding. Protein Eng *15*, 521-528.
22. Brandizzi, F., Hanton, S., DaSilva, L.L., Boevink, P., Evans, D., Oparka, K., Denecke, J., and Hawes, C. (2003). ER quality control can lead to retrograde transport from the ER lumen to the cytosol and the nucleoplasm in plants. Plant J *34*, 269-281.
23. Wang, R., and Brattain, M.G. (2007). The maximal size of protein to diffuse through the nuclear pore is larger than 60kDa. FEBS Lett *581*, 3164-3170.
24. Schoberer, J., Liebminger, E., Botchway, S.W., Strasser, R., and Hawes, C. (2013). Time-resolved fluorescence imaging reveals differential interactions of N-glycan processing enzymes across the Golgi stack in planta. Plant physiology *161*, 1737-1754.
25. Osterrieder, A., Carvalho, C.M., Latijnhouwers, M., Johansen, J.N., Stubbs, C., Botchway, S., and Hawes, C. (2009). Fluorescence lifetime imaging of interactions between golgi tethering factors and small GTPases in plants. Traffic *10*, 1034-1046.
26. Lev, S., Ben Halevy, D., Peretti, D., and Dahan, N. (2008). The VAP protein family: from cellular functions to motor neuron disease. Trends Cell Biol *18*, 282-290.
27. Nishimura, Y., Hayashi, M., Inada, H., and Tanaka, T. (1999). Molecular cloning and characterization of mammalian homologues of vesicle-associated membrane protein-associated (VAMP-associated) proteins. Biochem Biophys Res Commun *254*, 21-26.
28. Saravanan, R.S., Slabaugh, E., Singh, V.R., Lapidus, L.J., Haas, T., and Brandizzi, F. (2009). The targeting of the oxysterol-binding protein ORP3a to the endoplasmic reticulum relies on the plant VAP33 homolog PVA12. Plant J *58*, 817-830.
29. Loewen, C.J., and Levine, T.P. (2005). A highly conserved binding site in vesicle-associated membrane protein-associated protein (VAP) for the FFAT motif of lipid-binding proteins. J Biol Chem *280*, 14097-14104.
30. Deeks, M.J., Fendrych, M., Smertenko, A., Bell, K.S., Oparka, K., Cvrckova, F., Zarsky, V., and Hussey, P.J. (2010). The plant formin AtFH4 interacts with both actin and microtubules, and contains a newly identified microtubule-binding domain. J Cell Sci *123*, 1209-1215.

Figure 1

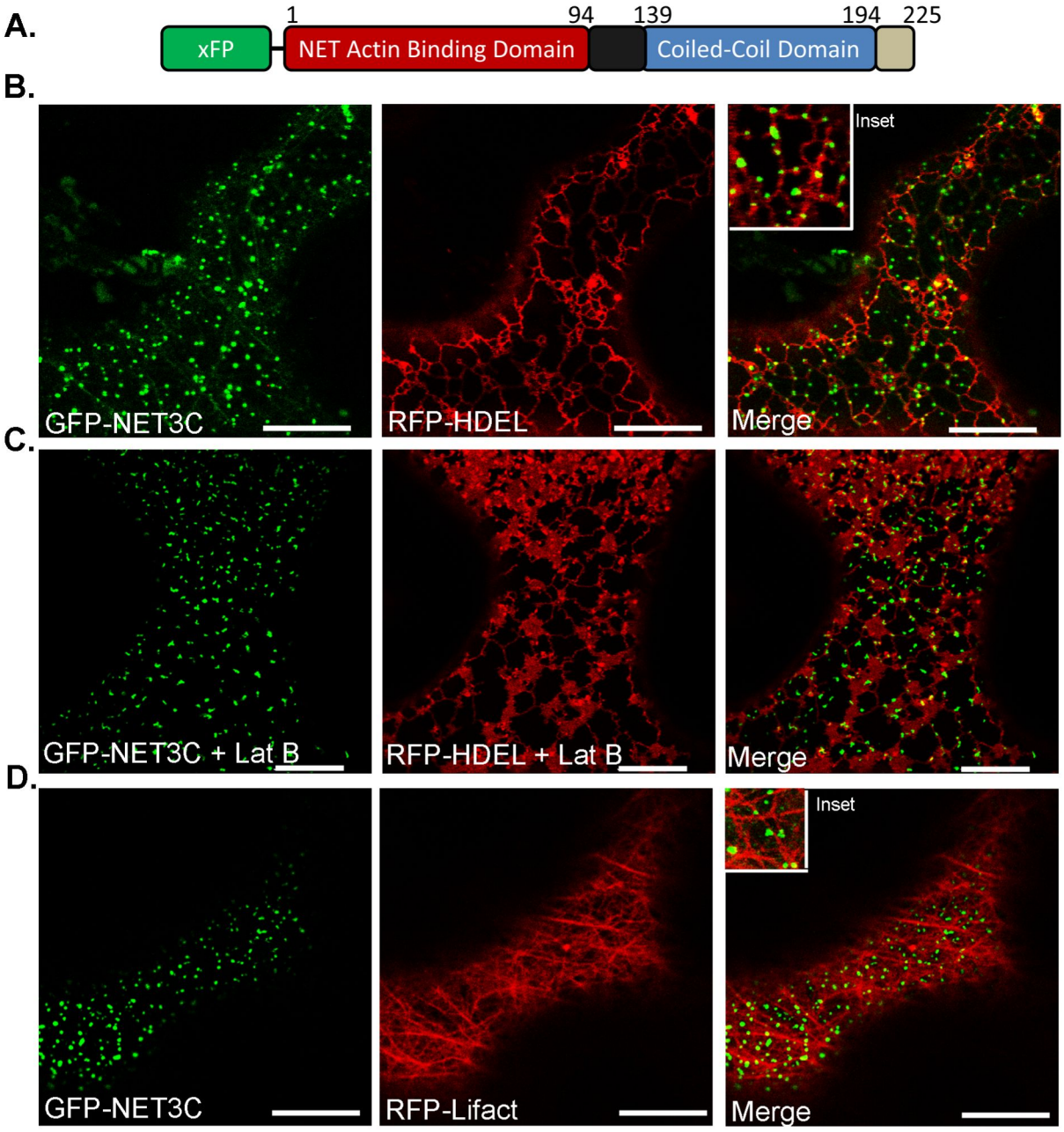

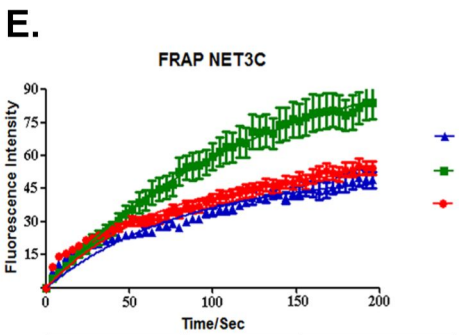

	Max Recovery (%)	Halftime of Recovery (s)
GFP-NET3C	44.55 ± 12.06	80.87 ± 37.9
GFP-NET3C + LatB	77.58 ± 18.5	91.27 ± 20.8
GFP-NET3C + Ory	43.62 ± 4.54	60.91 ± 24.49

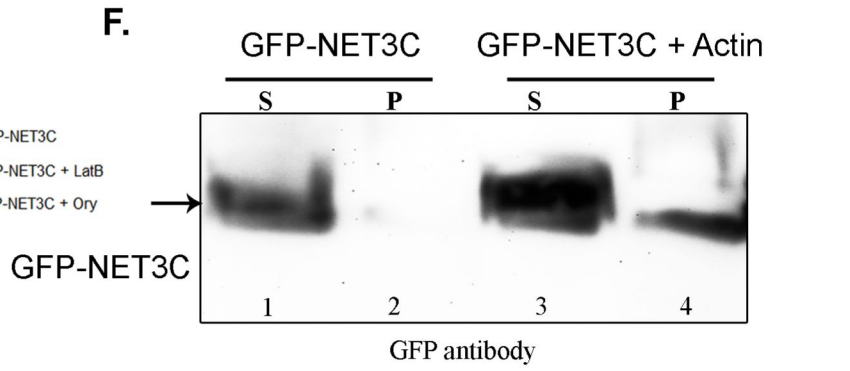

1. GFP-NET3C only, supernatant
2. GFP-NET3C only, pellet
3. GFP-NET3C + Actin, supernatant
4. GFP-NET3C + Actin, pellet

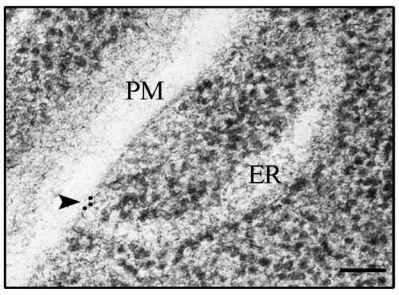

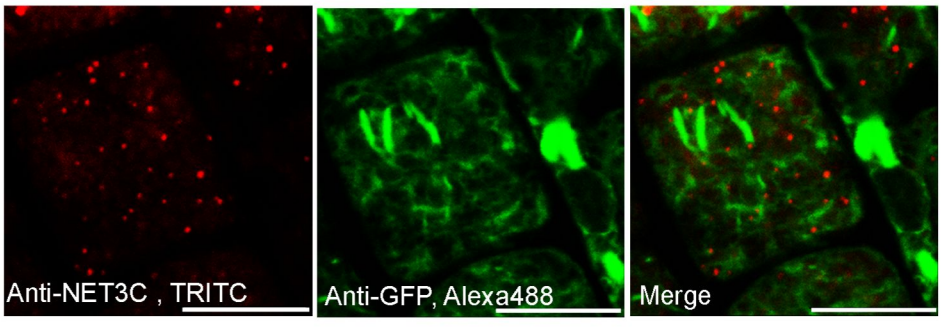

A.

B.

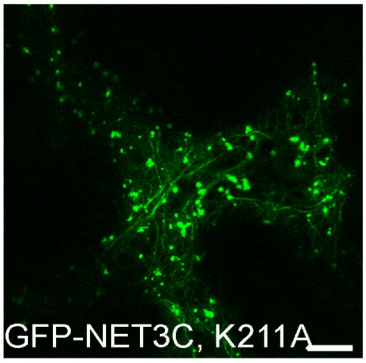

C.

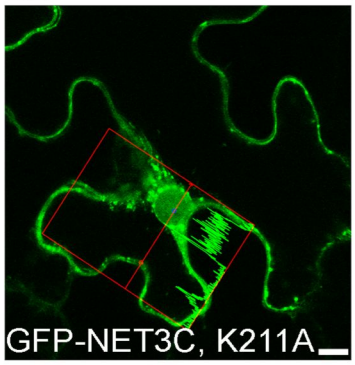

D.

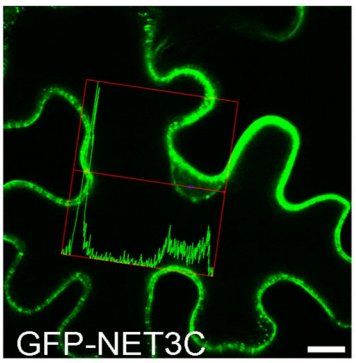

E.

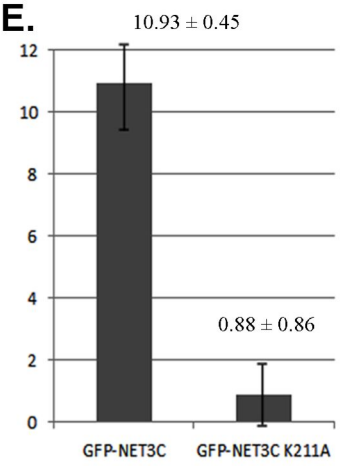

Flourescent intensity ratio
Peripheral/Nuclear

F.

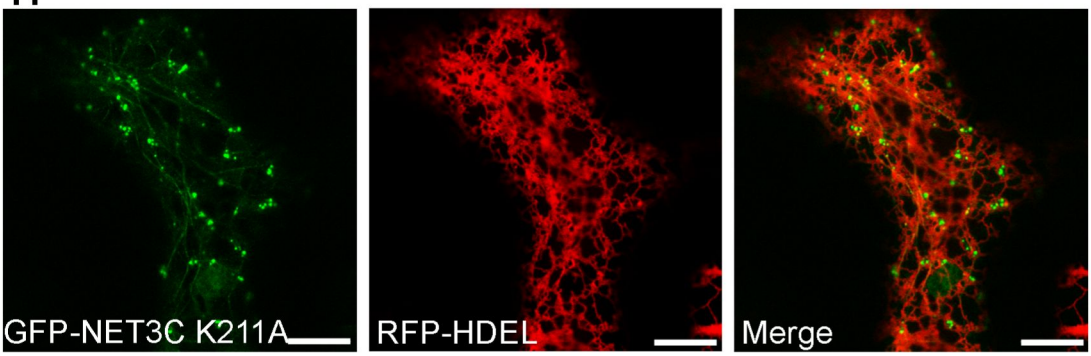

G.

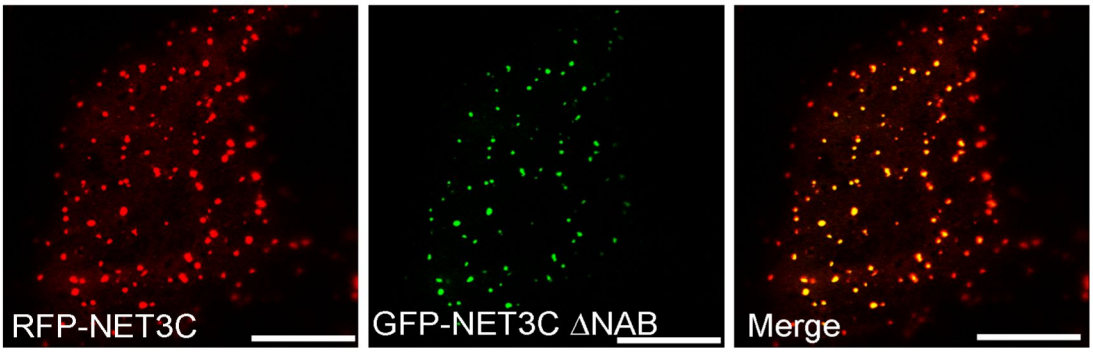

H.

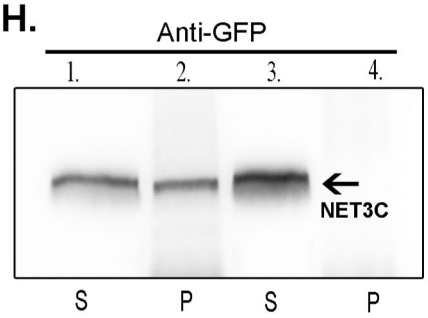

1. RFP-NET3C + GFP-NET3C, Supernatant
2. RFP-NET3C + GFP-NET3C, Pellet
3. GFP-NET3C, Supernatant
4. GFP-NET3C Pellet

I.

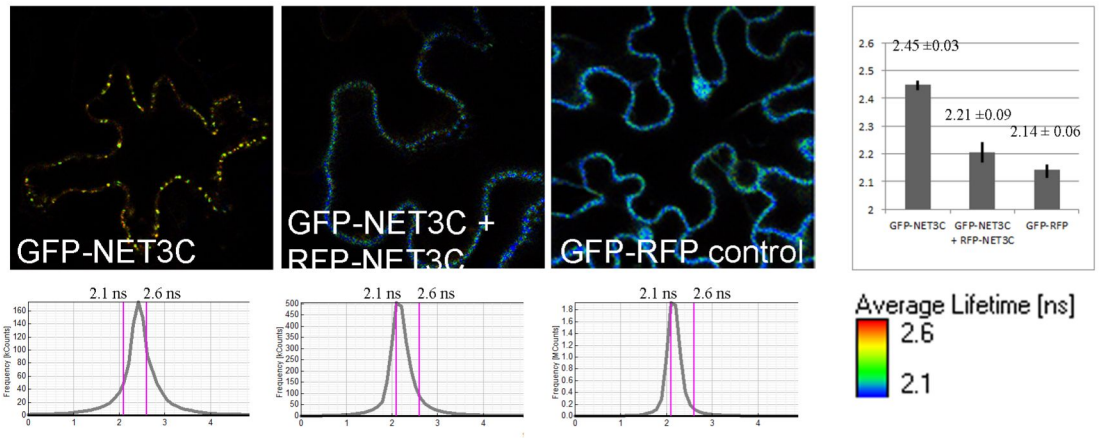

J.

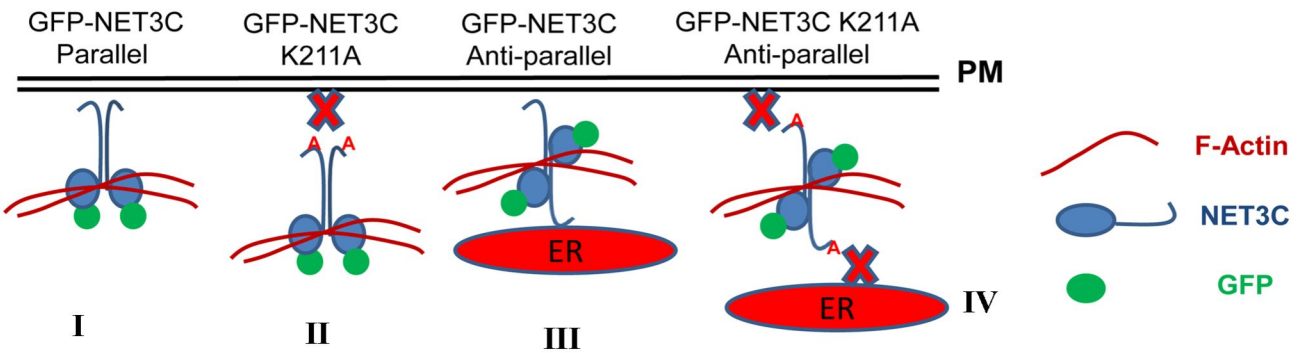

Figure 3

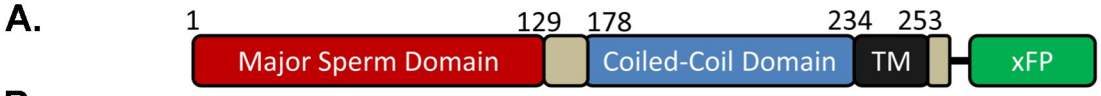

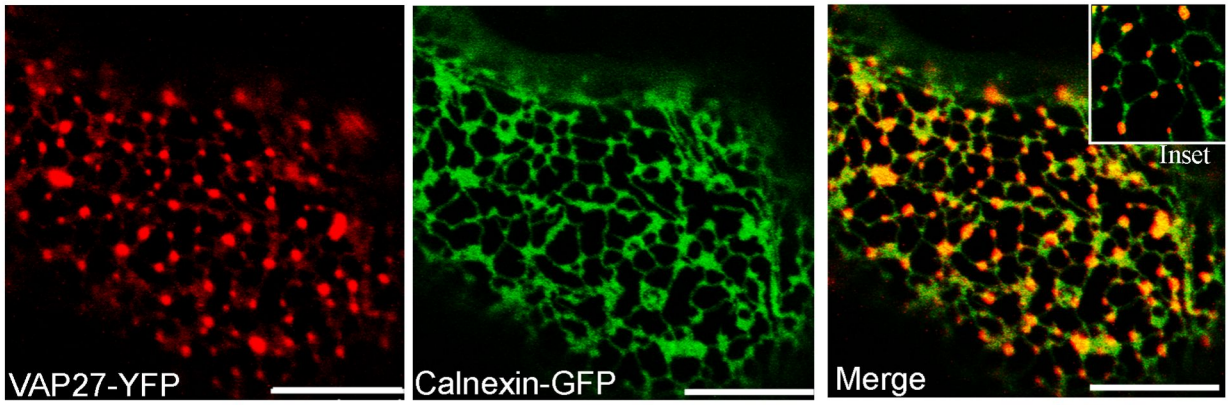

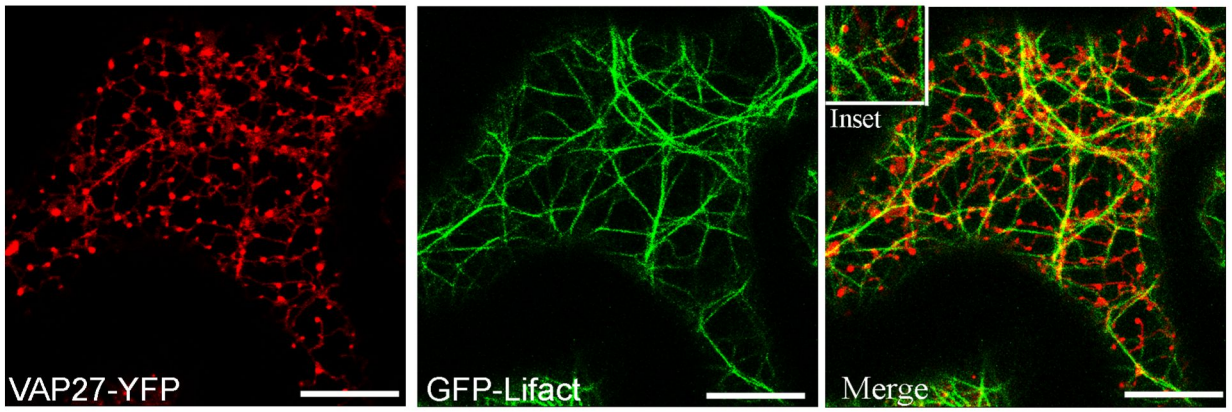

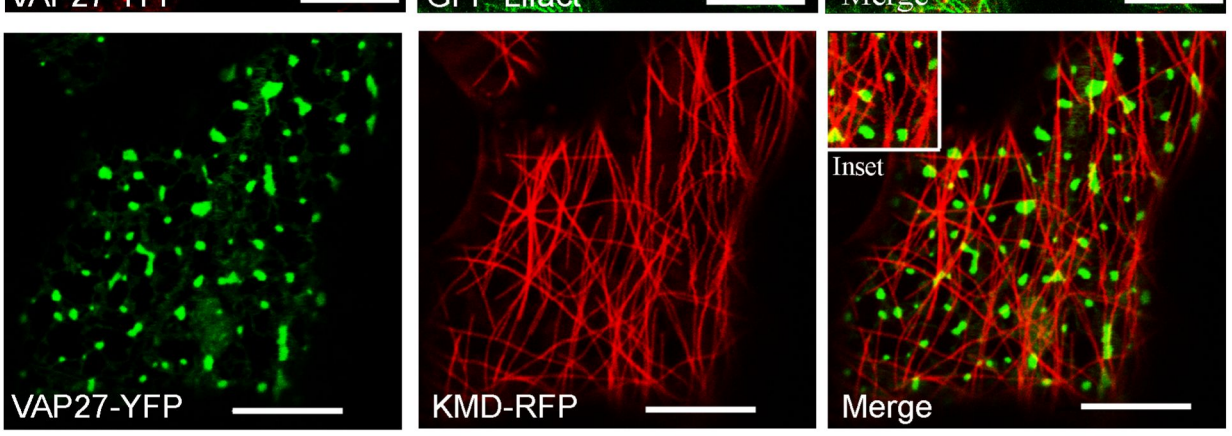

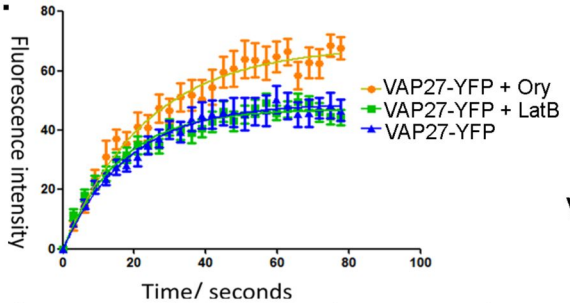

	Max Recovery (%)	Half Time (s)
VAP27-YFP	54.09 ± 12.55	14.95 ± 7.62
VAP27-YFP + LatB	49.87 ± 10.38	11.86 ± 4.03
VAP27-YFP + Ory	70.27 ± 16.33	18.16 ± 9.52

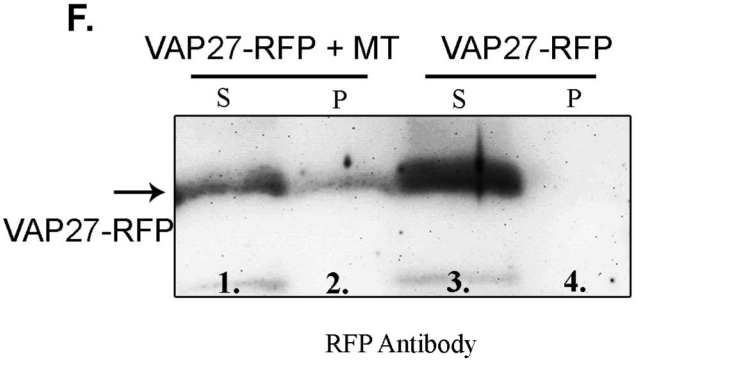

1. VAP27 + MT, supernatant
2. VAP27 + MT, pellet
3. VAP27 only, supernatant
4..VAP27 only, pellet

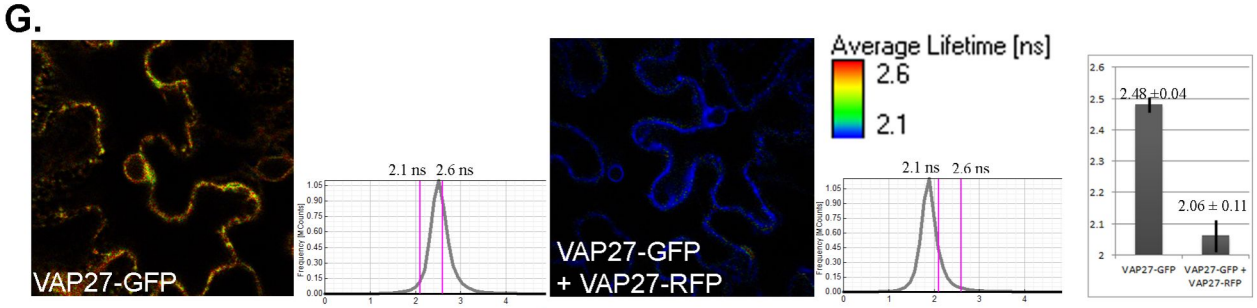

Figure 4

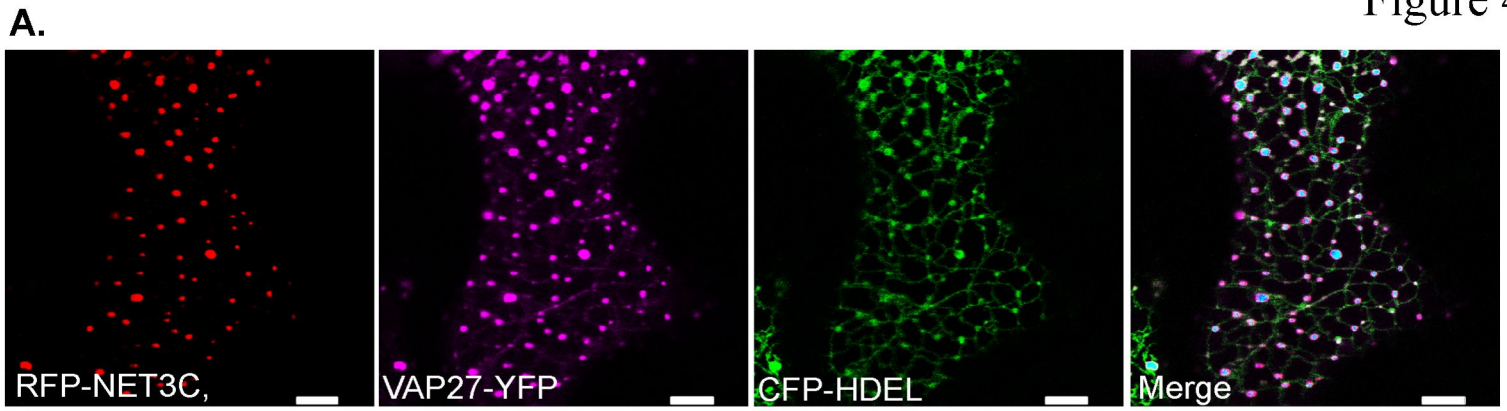
A.
RFP-NET3C,
VAP27-YFP
CFP-HDEL
Merge

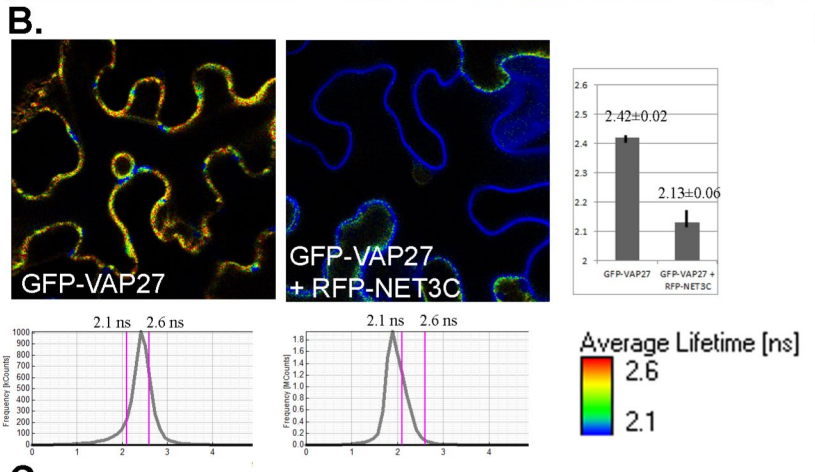
B.
GFP-VAP27
GFP-VAP27
+ RFP-NET3C
2.42±0.02
2.13±0.06
GFP-VAP27
GFP-VAP27 + RFP-NET3C
2.1 ns
2.6 ns
2.1 ns
2.6 ns
Average Lifetime [ns]
2.6
2.1

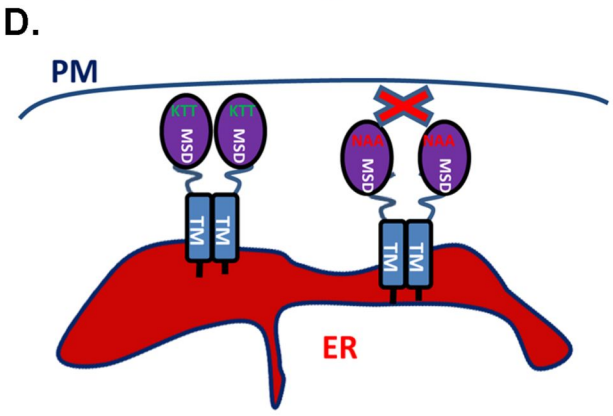
D.
PM
KTT
MSD
TM
NAA
ER

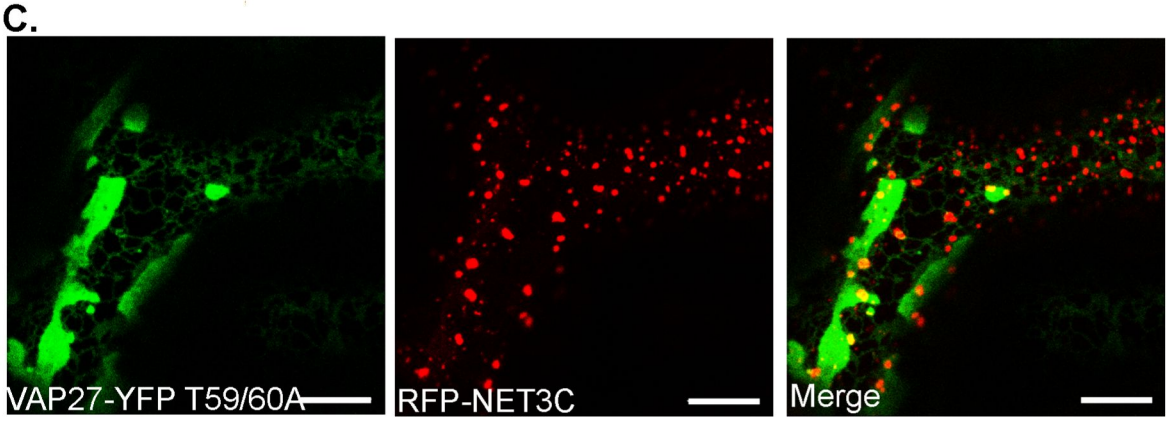
C.
VAP27-YFP T59/60A
RFP-NET3C
Merge

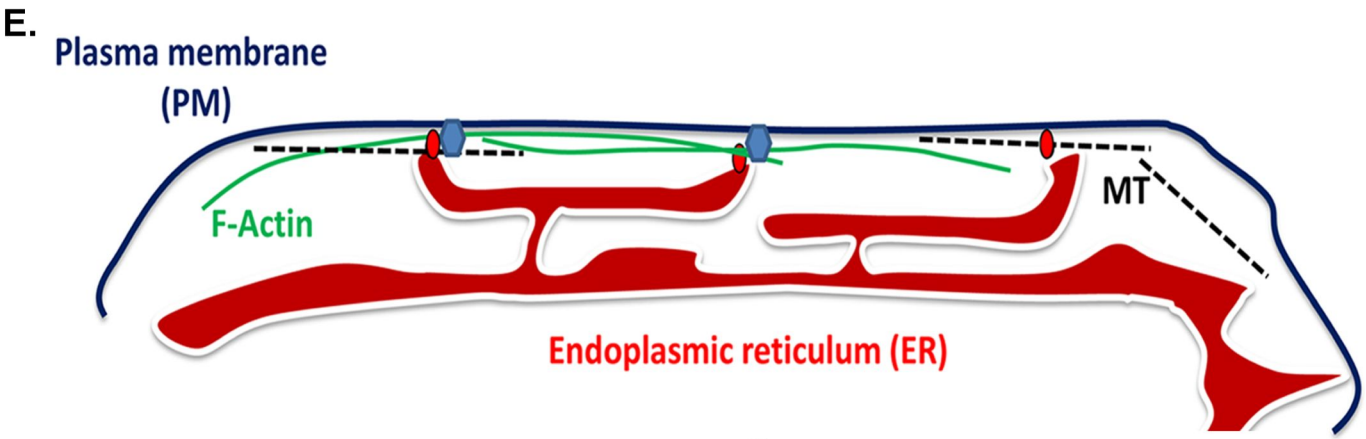
E.
Plasma membrane
(PM)
F-Actin
MT
Endoplasmic reticulum (ER)

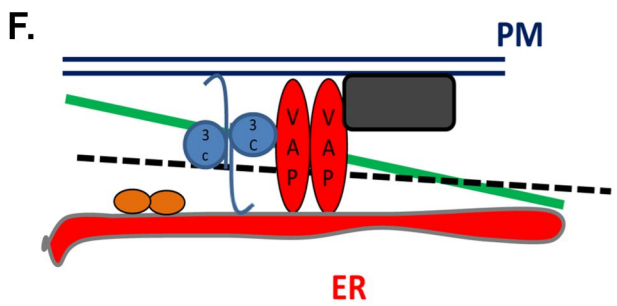
F.
PM
3 c
3 C
V A P
ER

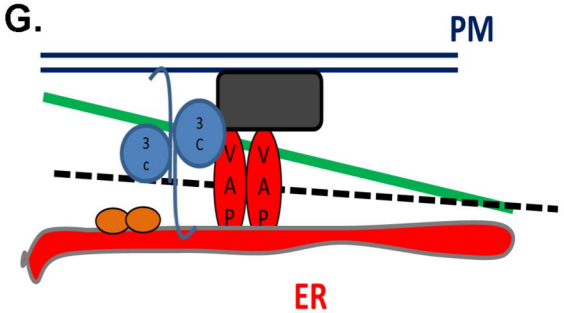
G.
PM
3 c
3 C
V A P
ER


Unknown ER proteins
Unknown PM proteins
F-Actin
Microtubules